Analysis of the roll properties of a tubular-type torsion beam suspension

K-J Mun[1], **T-J Kim**[1], and **Y-S Kim**[2*]
[1]R&D Center, Hwashin Co., Ltd, Yeongcheon, Geongbuk, Republic of Korea
[2]Department of Mechanical Engineering, Kyungpook National University, Buk-ku, Daegu, Republic of Korea

The manuscript was received on 3 April 2009 and was accepted after revision for publication on 13 July 2009.

DOI: 10.1243/09544070JAUTO1229

Abstract: Tubular-type torsion beam rear-suspension systems are widely used in small passenger cars owing to their compactness, light weight, and cost efficiency. It is already known that the roll behaviour of a torsion beam suspension system can be approximated to that of a semitrailing arm suspension system. By this kinematic assumption, analytical equations to obtain the roll centre height, roll steer, and roll camber have already been developed in terms of geometry points. Therefore, this paper proposes an analytical method to calculate the torsional stiffness of a tubular beam from its cross-section area based on the assumption that a tubular beam is a series connection of finite lengths with a constant cross-section. In addition, a potential energy method is proposed to calculate the roll stiffness of a tubular torsion beam suspension system based on considering the bushing stiffness and torsional stiffness of the tubular beam without the use of any commercial computer-aided engineering (CAE) software. The torsional stiffness and roll stiffness predicted using the proposed method showed errors of about 4 per cent and 3.3 per cent respectively, when compared with results from commercial CAE software.

Keywords: torsion beam suspension, tubular beam, shear centre, roll centre height, roll steer, roll camber, roll stiffness

1 INTRODUCTION

Torsion beam rear-suspension systems have recently been widely used for small passenger vehicles, because of various advantages, including a reduced weight, lower cost, and greater space efficiency, when compared with other types of suspension system [**1**]. A torsion beam rear-suspension system consists of two longitudinal trailing arms on the left and right sides and a torsion beam that is interconnected between the two trailing arms and other brackets for spring seats, dampers, spindles, and rubber bushings (Fig. 1). As such, the torsion beam provides the torsional and bending stiffness required for the suspension performance. Typically, there are two types of torsion beam: a V- or U-shaped open-section beam that is made by stamping a thick plate, and a hollow closed-section tubular beam made by pressing an original pipe; the latter type is more popular, as a tubular beam can replace many parts such as beam, torsion bar, and reinforcements for a V- or U-shaped beam. The geometric profile of a tubular beam generally consists of a constant section area, a transition area in which the section profile is changed along its distance, and a square-type section area at each end which is welded to the trailing arms, as shown in Fig. 2.

Nonetheless, despite the relatively simple structure of a torsion beam suspension system, many design variables need to be determined during the early design planning stage, e.g. predicting the effect of the design variables of the torsion beam suspension system on the vehicle handling performance using an ADAMS simulation [**2**, **3**] and other codes [**4**], considering the elastic deformation in a elasto-kinematic system with a component mode synthesis method. Yet, while such multi-body dynamic soft-

*Corresponding author: Department of Mechanical Engineering, Kyungpook National University, 1370 Sangyeok, Buk-ku, Daegu 702-701, Republic of Korea.
email: caekim@knu.ac.kr

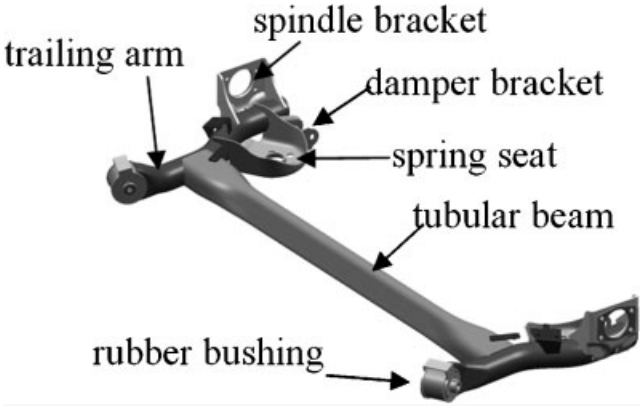

Fig. 1 Torsion beam-type rear suspension system

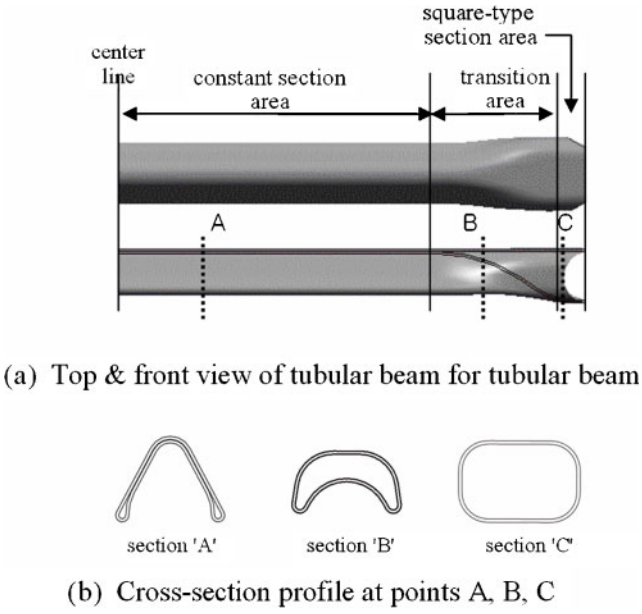

Fig. 2 Typical cross-section profile of a tubular beam

ware provides comparable results with test data [**5**, **6**], the whole process is time consuming, including meshing the torsion beam model using preprocessor software and making a modal neutral file using a finite element (FE) solver. Also, it requires specialized skills and knowledge. Thus, an alternative efficient technique is needed to obtain quick results, especially during the initial design planning stage when there are so many design variables to be determined. Sugiura *et al.* [**7**] have already developed an in-house design tool that can automatically generate a reduced stiffness matrix from a cross-section of a torsion beam drawn with a Microsoft Excel spreadsheet (using the Guyan reduction method), and then can calculate the compliance properties. Meanwhile, Lyu *et al.* [**8**] represented a torsion beam as the linkage of a lumped mass joined by non-linear bending–torsional springs which is calculated using non-linear FE simulations.

Satchell [**9**] proposed that the deformation behaviour of a torsion beam suspension system in a roll motion is similar to the kinematic motion of a semitrailing arm in which the line connecting the attachment of the rubber bushing and the shear centre of the torsion beam is the axis of rotation. This kinematic analogy assumption then allows prediction of the basic roll properties, such as the roll centre height, roll camber, roll steer, and roll stiffness of the torsion beam suspension, all of which are important factors affecting the vehicle-handling performance. Kang [**6**] also proposed kinematic expressions for the roll centre height, roll steer, roll camber, and roll stiffness as functions of the shear centre, hard points, spring stiffness, and torsional stiffness in the case of a V-shaped open-section beam; yet FE software is still needed to calculate the torsional stiffness, as there is no general analytical equation for the torsional stiffness of an arbitrary V-shaped beam, and there is no consideration of the rubber bushing stiffness.

Accordingly, this paper focuses on the roll properties of a tubular beam-type torsion beam suspension system. In the case of a tubular beam, the equations for the roll centre height, roll steer, and roll camber proposed by Kang [**6**] can be used. However, for the roll stiffness of a tubular beam, this paper presents a new analytical method using the beam geometry and rubber bushing data. First, an analytical method is proposed to calculate the torsional stiffness of a tubular beam from its cross-section area, based on the assumption in linear beam theory that a tubular beam is a series connection of finite lengths with a constant cross-section. Second, a potential energy method is proposed to calculate the roll stiffness of a tubular torsion beam suspension system based on considering the rubber bushing stiffness and torsional stiffness of the tubular beam.

To demonstrate the effectiveness of the proposed methods in this paper, the roll properties were calculated and the results were compared with those obtained using an MSC.ADAMS simulation.

2 TORSION BEAM KINEMATICS

In the case of a roll motion when both sides of the wheel centre move in the opposite direction with the same displacement, the behaviour of the torsion beam is equivalent to the kinematic motion of a semitrailing arm suspension system [**9**], as shown in Fig. 3. In the analogy of a semitrailing arm, since the

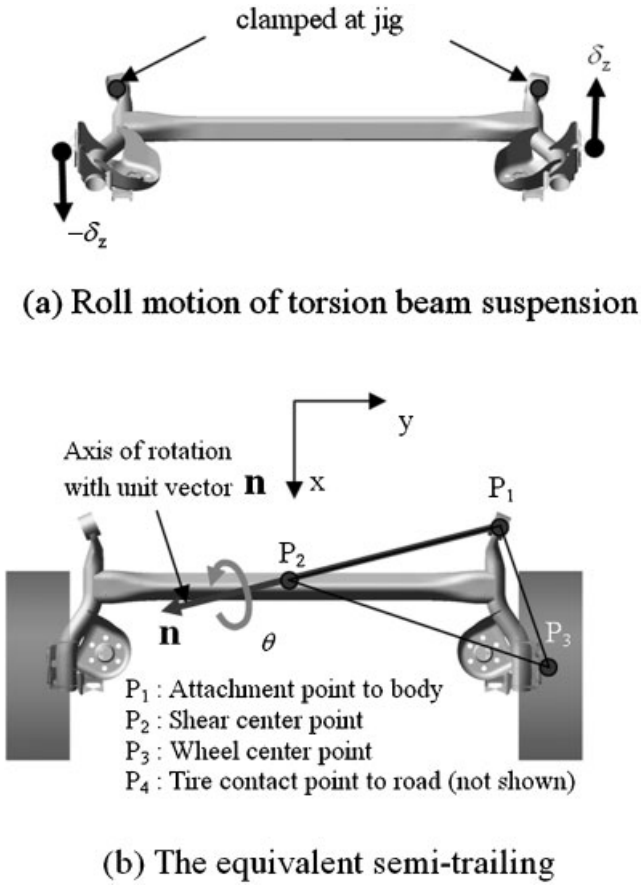

Fig. 3 Kinematic motion of the torsion beam in roll motion

line connecting the attachment point and the shear centre of the tubular beam is the axis of rotation, the kinematic motion of one side of the wheel rotates around this axis of rotation. Kinematic expressions for the related roll properties have already been developed by Kang [**6**] in the case of a V-shaped torsion beam. In this paper, these equations are expressed using Euler parameters and a transformation matrix.

The geometry points shown in Fig. 3(b) are used as the position vectors from the origin of the global coordinate in the following expressions. The directions of the x, y, and z axes in global coordinate are rearward, right, and vertical respectively, with respect to the driver in accordance with the car coordinate system of car maker.

2.1 Transformation matrix

To derive the equation, the local coordinate is set at point P_1 as the origin and parallel to the global coordinate in the initial condition ($\boldsymbol{P}_1$ is the distance of P_1 from the origin). According to the analogy of the semitrailing arm, the kinematic roll motion of torsion beam is expressed by the fact that half of the torsion beam and trailing arm is assumed to rotate by an angle θ around the axis of rotation with unit vector $\boldsymbol{n}$, in which the direction is from the attachment point P_1 to the shear centre P_2 of the tubular beam. The transformation matrix $\mathbf{A}$ can then be represented as the Euler parameters $\boldsymbol{p}$ [**10**] according to

$$\begin{aligned}\boldsymbol{n} &= \frac{\boldsymbol{P}_2 - \boldsymbol{P}_1}{|\boldsymbol{P}_2 - \boldsymbol{P}_1|} \\ &= [n_x, n_y, n_z]^{\mathrm{T}}\end{aligned} \tag{1}$$

$$\begin{aligned}\boldsymbol{p} &= [e_0, e_1, e_2, e_3]^{\mathrm{T}} \\ &= \left[\cos\left(\frac{\theta}{2}\right), n_x \sin\left(\frac{\theta}{2}\right), n_y \sin\left(\frac{\theta}{2}\right), n_z \sin\left(\frac{\theta}{2}\right)\right]^{\mathrm{T}}\end{aligned} \tag{2}$$

$$\begin{aligned}\mathbf{A} &= \begin{bmatrix} A_{11} & A_{12} & A_{13} \\ A_{21} & A_{22} & A_{23} \\ A_{31} & A_{32} & A_{33} \end{bmatrix} \\ &= \begin{bmatrix} e_0^2 + e_1^2 - e_2^2 - e_3^2 & 2(e_1e_2 - e_3e_0) & 2(e_1e_3 + e_2e_0) \\ 2(e_1e_2 + e_3e_0) & -e_1^2 + e_2^2 - e_3^2 + e_0^2 & 2(e_2e_3 - e_1e_0) \\ 2(e_1e_3 - e_2e_0) & 2(e_2e_3 + e_1e_0) & e_0^2 - e_1^2 - e_2^2 + e_3^2 \end{bmatrix}\end{aligned} \tag{3}$$

As a result, the local component vector $\boldsymbol{s}'$ for the local coordinate can be transformed into the global component vector $\boldsymbol{s}$ for the global coordinate as a function of the rotation angle θ according to

$$\boldsymbol{s} = \mathbf{A}\boldsymbol{s}' \tag{4}$$

2.2 Wheel centre motion

Define the local vector $\boldsymbol{s}'_3$ for the local x', y', z' coordinates, and the displacement $\boldsymbol{\delta}$ of the wheel centre as

$$\begin{aligned}\boldsymbol{s}'_3 &= \boldsymbol{P}_3 - \boldsymbol{P}_1 \\ &= \begin{bmatrix} s'_{3x} \\ s'_{3y} \\ s'_{3z} \end{bmatrix} \\ &= \begin{bmatrix} P_{3x} \\ P_{3y} \\ P_{3z} \end{bmatrix} - \begin{bmatrix} P_{1x} \\ P_{1y} \\ P_{1z} \end{bmatrix}\end{aligned} \tag{5}$$

$$\boldsymbol{\delta} = \begin{bmatrix} \delta_x & \delta_y & \delta_z \end{bmatrix}^{\mathrm{T}} = \boldsymbol{P}_1 + \mathbf{A}\boldsymbol{s}'_3 \tag{6}$$

The vertical component δ_z of the wheel centre then becomes

$$\begin{aligned}\delta_z &= A_{31}s'_{3x} + A_{32}s'_{3y} + A_{33}s'_{3z} + P_{1z} \\ &= 2(e_1e_3 - e_2e_0)s'_{3x} + 2(e_2e_3 + e_1e_0)s'_{3y} \\ &\quad + \left(-e_1^2 - e_2^2 + e_3^2 + e_0^2\right)s'_z + P_{1z}\end{aligned} \tag{7}$$

The derivative δ_z with respect to θ at $\theta = 0$ is

$$\left.\frac{\mathrm{d}\delta_z}{\mathrm{d}\theta}\right|_{\theta=0} = n_x s'_{3y} - n_y s'_{3x} \tag{8}$$

2.3 Roll steer and roll camber

Define the local vector $\boldsymbol{s}'_{\mathrm{p}}$ as the unit vector of the spindle axis, i.e. $\boldsymbol{s}'_{\mathrm{p}} = [0 \quad 1 \quad 0]^{\mathrm{T}}$ in Fig. 4(a). From equations (3) and (4), the global vector then becomes

$$\begin{aligned}\boldsymbol{s}_{\mathrm{p}} &= \mathbf{A}\boldsymbol{s}'_{\mathrm{p}} \\ &= \begin{bmatrix} s_{\mathrm{p}x} \\ s_{\mathrm{p}y} \\ s_{\mathrm{p}z} \end{bmatrix} \\ &= \begin{bmatrix} 2(e_1e_2 - e_3e_0) \\ -e_1^2 + e_2^2 - e_3^2 + e_0^2 \\ 2(e_2e_3 + e_1e_0) \end{bmatrix}\end{aligned} \tag{9}$$

The toe angle θ_{toe} and camber angle θ_{camb}, shown in Fig. 4(b), can be expressed as

$$\theta_{\mathrm{toe}} = -\tan^{-1}\left(\frac{s_{\mathrm{p}x}}{s_{\mathrm{p}y}}\right) \tag{10}$$

$$\theta_{\mathrm{camb}} = -\tan^{-1}\left(\frac{s_{\mathrm{p}z}}{\sqrt{s_{\mathrm{p}x}^2 + s_{\mathrm{p}y}^2}}\right) \tag{11}$$

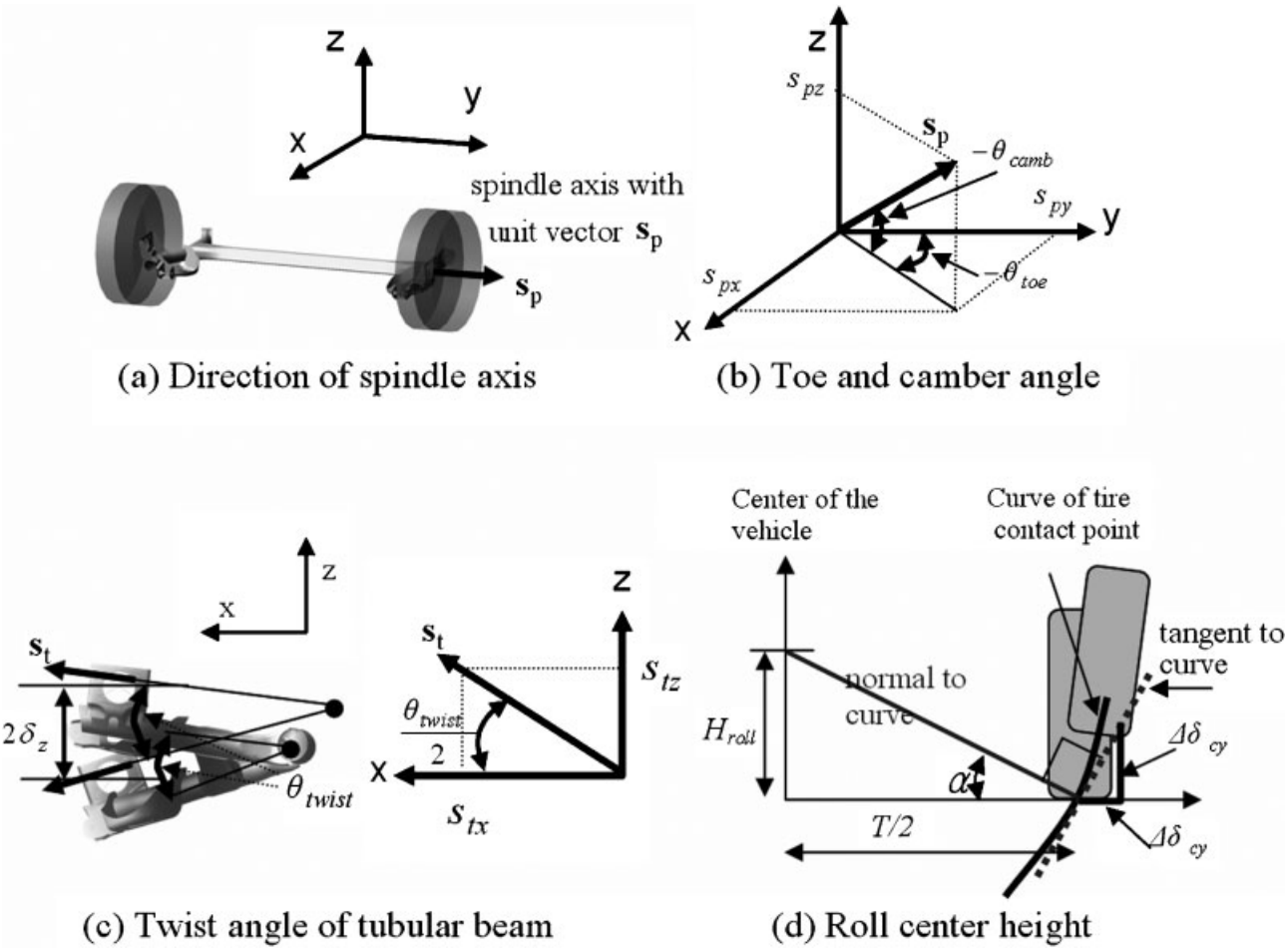

Fig. 4 Definition of parameters

The derivative of the toe angle θ_{toe} with respect to θ at $\theta = 0$ becomes

$$\left.\frac{\mathrm{d}\theta_{\text{toe}}}{\mathrm{d}\theta}\right|_{\theta=0} = \left.\frac{-1}{\sqrt{1+\left(s_{\text{px}}/s_{\text{py}}\right)^2}}\right|_{\theta=0} \left.\frac{\mathrm{d}}{\mathrm{d}\theta}\left(\frac{s_{\text{px}}}{s_{\text{py}}}\right)\right|_{\theta=0} = n_z \tag{12}$$

From equations (8) and (12), the roll steer, defined as the derivative of the toe angle with respect to δ_z, is

$$\left.\frac{\mathrm{d}\theta_{\text{toe}}}{\mathrm{d}\delta_z}\right|_{\theta=0} = \left.\frac{\mathrm{d}\theta_{\text{toe}}}{\mathrm{d}\theta}\right|_{\theta=0} \left(\left.\frac{\mathrm{d}\delta_z}{\mathrm{d}\theta}\right|_{\theta=0}\right)^{-1} = \frac{n_z}{n_x s'_{3y} - n_y s'_{3x}} \tag{13}$$

According to equation (13), the sign of the numerator term determines the roll understeer or oversteer tendency. Thus, for a car with a rear torsion beam suspension to have a roll understeer tendency, i.e. for the toe angle to be toe-in (= positive toe angle) while the wheel centre moves vertically upwards, the numerator term should be positive, which means that the shear centre should be positioned above the attachment of the rubber bushing.

Next, the roll camber, defined as the derivative of the camber angle with respect to θ at $\theta = 0$, is determined via the same process as in the case of the roll steer according to

$$\left.\frac{\mathrm{d}\theta_{\text{camb}}}{\mathrm{d}\theta}\right|_{\theta=0} = -n_x \tag{14}$$

$$\left.\frac{\mathrm{d}\theta_{\text{camb}}}{\mathrm{d}\delta_z}\right|_{\theta=0} = \left.\frac{\mathrm{d}\theta_{\text{camb}}}{\mathrm{d}\theta}\right|_{\theta=0} \left(\left.\frac{\mathrm{d}\delta_z}{\mathrm{d}\theta}\right|_{\theta=0}\right)^{-1} = \frac{-n_x}{n_x s'_{3y} - n_y s'_{3x}} \tag{15}$$

According to equation (15), the roll camber always has a negative value.

2.4 Twist angle of the torsion beam

Define the local vector $\boldsymbol{s}'_{\text{t}}$ as the longitudinal unit vector $\boldsymbol{s}'_{\text{t}} = [1 \quad 0 \quad 0]^{\text{T}}$, and then the global vector $\boldsymbol{s}_{\text{t}}$ becomes

$$\boldsymbol{s}_{\text{t}} = \mathbf{A}\boldsymbol{s}'_{\text{t}} = \begin{bmatrix} s_{\text{tx}} \\ s_{\text{ty}} \\ s_{\text{tz}} \end{bmatrix} = \begin{bmatrix} e_0^2 + e_1^2 - e_2^2 - e_3^2 \\ 2(e_1 e_2 + e_3 e_0) \\ 2(e_1 e_3 - e_2 e_0) \end{bmatrix} \tag{16}$$

The twist angle θ_{twist} of the beam during the roll motion in Fig. 4(c) is then defined as

$$\theta_{\text{twist}} = 2\tan^{-1}\left(\frac{s_{\text{tz}}}{s_{\text{tx}}}\right) \tag{17}$$

and the derivative of the twist angle with respect to θ at $\theta = 0$ is

$$\left.\frac{\mathrm{d}\theta_{\text{twist}}}{\mathrm{d}\theta}\right|_{\theta=0} = \left.\frac{2}{\sqrt{1+\left(s_{\text{tz}}/s_{\text{tx}}\right)^2}}\right|_{\theta=0} \left.\frac{\mathrm{d}}{\mathrm{d}\theta}\left(\frac{s_{\text{tz}}}{s_{\text{tx}}}\right)\right|_{\theta=0} = -2n_y \tag{18}$$

Also, the derivative of the twist angle of the tubular beam with respect to the vertical displacement of the wheel centre is

$$\left.\frac{\mathrm{d}\theta_{\text{twist}}}{\mathrm{d}\delta_z}\right|_{\theta=0} = \left.\frac{\mathrm{d}\theta_{\text{twist}}}{\mathrm{d}\theta}\right|_{\theta=0} \left(\left.\frac{\mathrm{d}\delta_z}{\mathrm{d}\theta}\right|_{\theta=0}\right)^{-1} = \frac{-2n_y}{n_x s'_{3y} - n_y s'_{3x}} \tag{19}$$

According to equation (19), if the shear centre of the tubular beam or the position of the tubular beam is located forwards, the component of '$-n_y$' and the torsional angle rate become larger.

2.5 Roll centre height

The roll centre is an idealized point in the transverse vertical plane through any pair of wheel centres at which lateral forces may be applied to the sprung mass without producing any suspension roll [**11**]. Thus, the roll centre height is defined as the height of the point from the ground at which the normal vector for the curve of the tyre contact intersects at the centre of the vehicle [**12**], as shown in Fig. 4(d).

If the curve of the tyre contact point $(\delta_{\text{cy}}, \delta_{\text{cz}})$ is known, the angle α of the normal vector for the curve of the tyre contact point is

$$\tan\alpha = \left.\frac{\mathrm{d}\delta_{\text{cy}}}{\mathrm{d}\delta_{\text{cz}}}\right|_{\theta=0} \tag{20}$$

and the roll centre height H_{roll} is then expressed as the function of the wheel tread T and angle α according to

$$H_{\text{roll}} = \frac{T}{2}\tan\alpha \tag{21}$$

To calculate the curve of the tyre contact point, let the local vector $\boldsymbol{s}'_4$ be

$$\boldsymbol{s}'_4 = \boldsymbol{P}_4 - \boldsymbol{P}_1 = \begin{bmatrix} s'_{4x} \\ s'_{4y} \\ s'_{4z} \end{bmatrix} = \begin{bmatrix} P_{4x} \\ P_{4y} \\ P_{4z} \end{bmatrix} - \begin{bmatrix} P_{1x} \\ P_{1y} \\ P_{1z} \end{bmatrix} \tag{22}$$

Then the global vector for the tyre contact point becomes

$$\boldsymbol{\delta}_c = \begin{bmatrix} \delta_{cx} & \delta_{cy} & \delta_{cz} \end{bmatrix}^T = \boldsymbol{P}_1 + \mathbf{A}\boldsymbol{s}'_4 \tag{23}$$

The lateral and vertical components of the tyre contact point in equation (23) are

$$\delta_{cy} = A_{21}s'_{4x} + A_{22}s'_{4y} + A_{23}s'_{4z} + P_{1y} \tag{24}$$

$$\delta_{cz} = A_{31}s'_{4x} + A_{32}s'_{4y} + A_{33}s'_{4z} + P_{1z} \tag{25}$$

The derivatives of equations (24) and (25) with respect to θ at $\theta = 0$ are

$$\left.\frac{\mathrm{d}\delta_{cy}}{\mathrm{d}\theta}\right|_{\theta=0} = n_z s'_{4x} - n_x s'_{4z} \tag{26}$$

$$\left.\frac{\mathrm{d}\delta_{cz}}{\mathrm{d}\theta}\right|_{\theta=0} = -n_y s'_{4x} + n_x s'_{4y} \tag{27}$$

From equations (20), (21), (26), and (27), the roll centre height can be expressed as

$$\tan\alpha = \left.\frac{\mathrm{d}\delta_{cy}}{\mathrm{d}\delta_{cz}}\right|_{\theta=0} = \left.\frac{\mathrm{d}\delta_{cy}/\mathrm{d}\theta}{\mathrm{d}\delta_{cz}/\mathrm{d}\theta}\right|_{\theta=0} = \frac{n_z s'_{4x} - n_x s'_{4z}}{n_x s'_{4y} - n_y s'_{4x}} \tag{28}$$

$$H_{roll} = \frac{T}{2}\tan\alpha = \frac{T}{2}\frac{n_z s'_{3x} - n_x s'_{3z}}{n_x s'_{3y} - n_y s'_{3x}} \tag{29}$$

2.6 Torsional stiffness of the tubular beam

To calculate the roll stiffness contribution of a tubular torsion beam, the torsional stiffness of the tubular beam has to be calculated. While a more precise torsional stiffness can be calculated using FE software, this paper proposes an analytical method using linear beam theory and geometry data to calculate the torsional stiffness without the help of FE software. First, assume a beam of length L with a constant closed cross-section that is twisted at both ends, as shown in Fig. 5(a), where A is the shaded area within the midline of the closed cross-section of the beam and S is the total length of the boundary. According to linear beam theory [**13**], under the assumption of a constant shear flow, the torsional stiffness of a beam is expressed as

$$K_t = \frac{\text{torque}}{\theta} = \frac{4A^2Gt}{SL} \tag{30}$$

where G and t are the shear modulus and thickness respectively of the beam.

In the case of a tubular beam, the cross-section area of the midline is necessarily changed along its distance from the centre (see Figs 2 and 8). Thus, to calculate the torsional stiffness of a tubular beam, this paper assumed that a tubular beam is a series connection of finite lengths Δ_i within a constant section, as shown in Fig. 5(b).

The equivalent torsional stiffness K_{tors} of a tubular beam is then approximated as

$$\frac{1}{K_{tors}} = \sum_i \frac{1}{K_{ti}} = \sum_i \frac{S_i\Delta_i}{4A_i^2Gt}$$
$$K_{tors} = \left(\sum_i \frac{1}{K_{ti}}\right)^{-1} = \left(\sum_i \frac{S_i\Delta_i}{4A_i^2Gt}\right)^{-1} \tag{31}$$

2.7 Roll stiffness of the torsion beam suspension

Assume a torsion beam suspension with rubber bushing that is twisted by two external forces of the same magnitude and yet opposite vertical direction

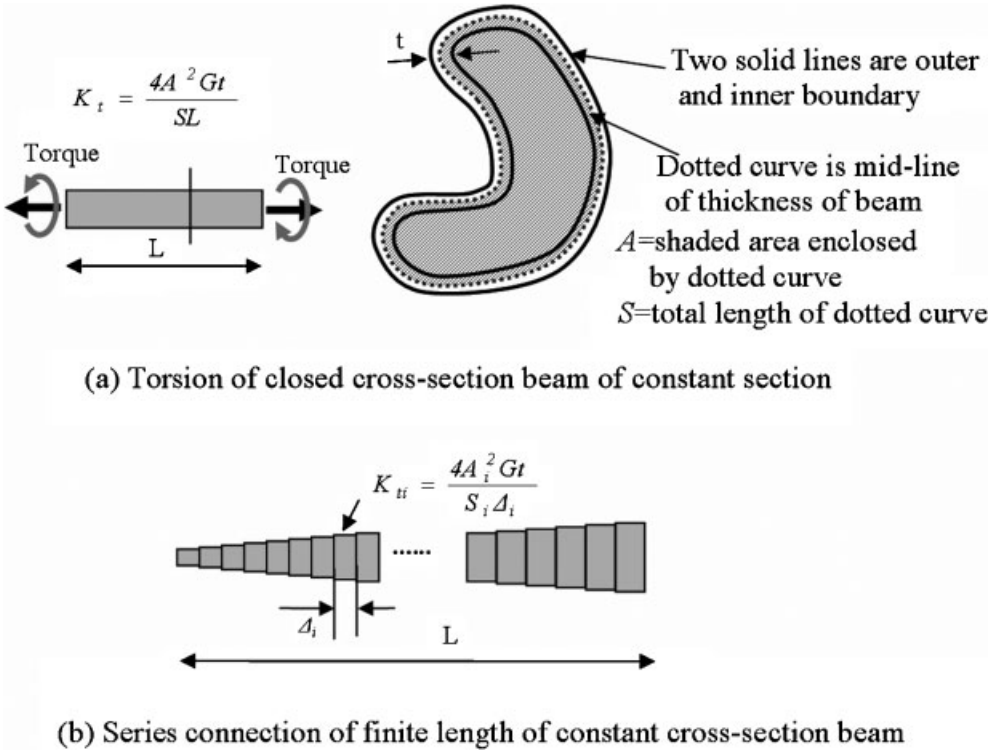

Fig. 5 Torsion of the closed cross-section beam with variable section area

forces. As such, the work performed by the two external forces is equal to the sum of the elastic torsional energy in the tubular beam and the torsional and conical energy in the rubber bushings attached to the body. The elastic effect of the trailing arm is not considered here, as the trailing arm itself is very stiff when compared with the other components.

In most cases, the rubber bushing is tilted at a certain angle to increase the understeer tendency, as in Fig. 6(a); however, in this paper a zero tilting angle is assumed. Also in this paper, the elastic effect of rubber bushing is represented by two stiffnesses: torsional stiffness and conical stiffness. The torsional stiffness K_{btz} is related to the rotation about the radial direction, and the conical stiffness K_{btc} is related to the rotation about the axial direction of the bushing in Figs 6(b) and (c).

To consider the effect of the stiffness of the rubber bushing in the roll stiffness, this paper assumes that the torsional angle θ_{btz} of the rubber bushing is equal to half the twist angle of the beam, while the conical angle θ_{btc} of the rubber bushing is the same as the camber angle of the wheel. Thus

$$\theta_{btz} = \frac{\theta_{twist}}{2} \tag{32}$$

$$\theta_{btc} = \theta_{camb} \tag{33}$$

Define the magnitude of the external force at both wheel centres as P. This paper assumes that the potential energy Π_p of the torsion beam suspension in a roll motion is the sum of the components of the energies of the tubular beam, rubber bushing, and external forces as given by

$$\Pi_p = \frac{1}{2}K_{tors}\theta_{twist}^2 + 2\frac{1}{2}K_{btz}\theta_{btz}^2 + 2\frac{1}{2}K_{btc}\theta_{btc}^2 - 2P\delta_z \tag{34}$$

In a stationary condition, the potential energy should meet the condition

$$\begin{aligned}\frac{d\Pi_p}{d\delta_z} &= 0\\ &= K_{tors}\theta_{twist}\frac{d\theta_{twist}}{d\delta_z} + 2K_{btz}\theta_{btz}\frac{d\theta_{btz}}{d\delta_z}\\ &\quad + 2K_{btc}\theta_{btc}\frac{d\theta_{btc}}{d\delta_z} - 2P\,d\delta_z\end{aligned} \tag{35}$$

In the linear region, the relations between the torsional angles of the tubular beam and rubber bushing and the vertical displacement of the wheel centre are expressed as

$$\theta_{twist} = \frac{d\theta_{twist}}{d\delta_z}\delta_z \tag{36}$$

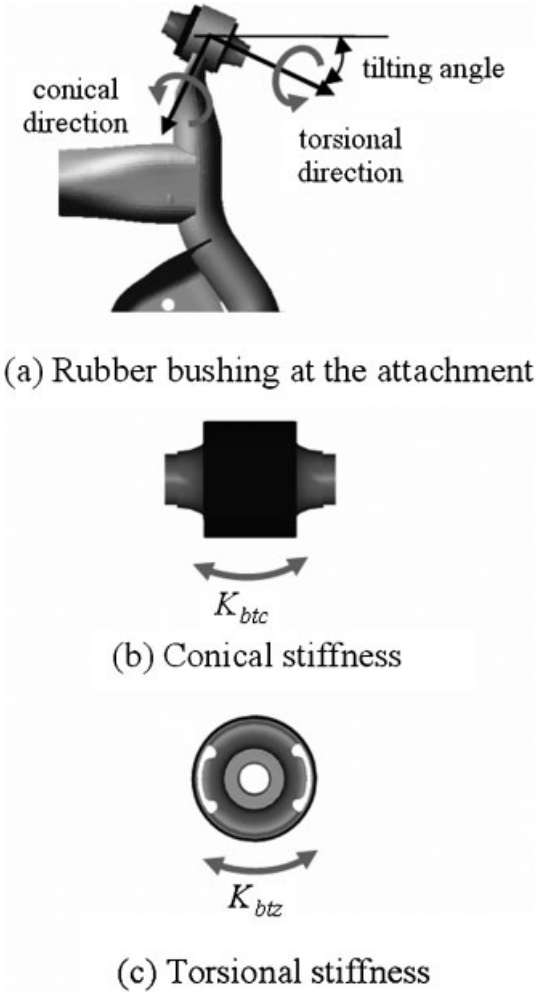

Fig. 6 Torsional and conical stiffnesses of the rubber bushing

$$\theta_{\mathrm{btz}} = \frac{\mathrm{d}\theta_{\mathrm{btz}}}{\mathrm{d}\delta_z}\delta_z = \frac{1}{2}\frac{\mathrm{d}\theta_{\mathrm{twist}}}{\mathrm{d}\delta_z}\delta_z \tag{37}$$

$$\theta_{\mathrm{btc}} = \frac{\mathrm{d}\theta_{\mathrm{camb}}}{\mathrm{d}\delta_z}\delta_z \tag{38}$$

From equations (35) to (38), the expression

$$\left[K_{\mathrm{tors}}\left(\frac{\mathrm{d}\theta_{\mathrm{twist}}}{\mathrm{d}\delta_z}\right)^2 + 2K_{\mathrm{btz}}\left(\frac{\mathrm{d}\theta_{\mathrm{btz}}}{\mathrm{d}\delta_z}\right)^2 + 2K_{\mathrm{btc}}\left(\frac{\mathrm{d}\theta_{\mathrm{btc}}}{\mathrm{d}\delta_z}\right)^2\right]\delta_z - 2P = 0 \tag{39}$$

is obtained.

From equation (39), the equivalent spring stiffness K_{eq} at the wheel centre is defined as

$$K_{\mathrm{eq}} = \frac{P}{\delta_z} = \frac{1}{2}\left[K_{\mathrm{tors}}\left(\frac{\mathrm{d}\theta_{\mathrm{twist}}}{\mathrm{d}\delta_z}\right)^2 + 2K_{\mathrm{btz}}\left(\frac{\mathrm{d}\theta_{\mathrm{twist}}}{\mathrm{d}\delta_z}\right)^2 + 2K_{\mathrm{btc}}\left(\frac{\mathrm{d}\theta_{\mathrm{camb}}}{\mathrm{d}\delta_z}\right)^2\right] \tag{40}$$

where the squared terms in equation (40) are given by equations (19) and (15) respectively.

The roll stiffness K_{roll} of a tubular beam is expressed as a function of the wheel tread T and the equivalent spring stiffness K_{eq} according to

$$K_{\mathrm{roll}} = \frac{1}{2}K_{\mathrm{eq}}T^2 \tag{41}$$

2.8 Shear centre of the closed cross-section beam

When two shear forces V_x and V_z are acting on the shear centre of a closed cross-section beam, as shown in Fig. 7, the shear flow q_{s} generated along the boundary is defined [**14–16**] as

$$q_{\mathrm{s}} = \frac{V_z I_{xz} - V_x I_{xx}}{I_{xx}I_{zz} - I_{xz}^2}\int tx\cdot \mathrm{d}s + \frac{V_x I_{xz} - V_z I_{zz}}{I_{xx}I_{zz} - I_{xz}^2}\int tz\cdot ds + q_{\mathrm{s},0} \tag{42}$$

The first two terms on the right-hand side represent the shear flow in the open section loaded through the shear centre, and the last term is the shear flow at $s = 0$.

Based on the shear forces at the shear centre, the torsional angle of the beam is zero, and the moments generated by the shear forces and shear flow are in a state of equilibrium. As such, the two equations

$$\frac{\mathrm{d}\theta}{\mathrm{d}z} = \frac{1}{2A}\oint\frac{q_{\mathrm{s}}}{Gt}\,\mathrm{d}s = 0 \tag{43}$$

$$V_z c_x - V_x c_z = \oint q_{\mathrm{s}} r\,\mathrm{d}s \tag{44}$$

should hold.

First, set $V_x = 1$ and $V_z = 0$. By putting equation (43) into equation (44), $q_{\mathrm{s},0}$ can be obtained; then equations (43) and (44) can be used to obtain the shear centre component c_z.

Next, set $V_x = 0$ and $V_z = 1$. Following the same process as explained above, the shear centre com-

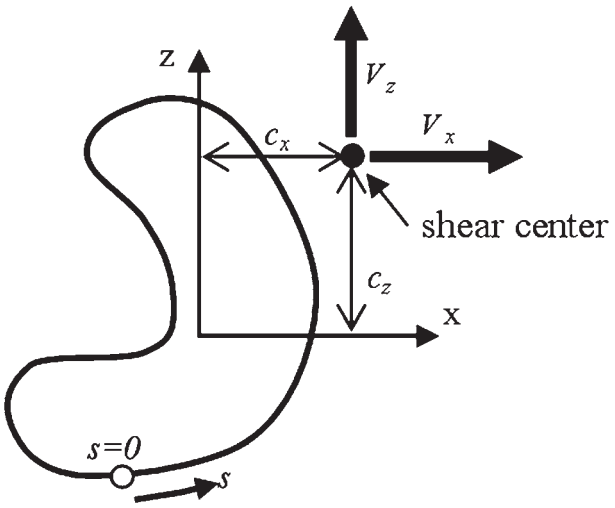

Fig. 7 Shear forces on the shear centre of the beam

ponent c_x can then be obtained. This paper used the FORTRAN programming language [**17**] to calculate the shear centre based on the algorithm in equations (42) to (44).

3 CASE STUDY

To validate the analytical method proposed in this paper, the analytical results were compared with the results from an MSC.ADAMS simulation.

3.1 Application model

The geometry data including the diameter and thickness of the original tubular beam are given in Table 1, while the cross-section areas enclosed by the midline of the thickness with respect to the distance from the centre of the tubular beam are shown in Fig. 8. The section areas were measured at 10 mm width, and the intermediate area was interpolated linearly.

In the case of the ADAMS model, the torsion beam was represented by the flexible body model shown in Fig. 9. ADAMS uses the orthogonalized Craig–Bampton modes which are stored in the modal neutral file for ADAMS simulations [**18**]. The first eigenvalue in the modal neutral file was 25.65 Hz.

The torsion beam suspension was fixed to the ground via a rubber bushing that was represented using the linear stiffness and mounted at the actual tilted angle.

The linear stiffness of the rubber bushing used in the ADAMS model was as follows: radial stiffness, 148.8 kgf/mm and 179.5 kgf/mm in the soft and hard directions, respectively; axial stiffness, 41.0 kgf/mm; conical stiffness, 20 053.52 kgf mm/rad; and torsional stiffness, 30 538.65 kgf mm/rad.

3.2 Validation of the analytical equation

The shear centre, calculated numerically using a FORTRAN program, is shown with the tubular beam cross-section shape in Fig. 10. The equation results for the roll steer, roll camber, and roll centre height are compared with the ADAMS simulation results in Table 2, including the twist angle rate. Except for the roll steer, the roll camber and roll centre height showed good agreement between the two methods.

The result of torsional stiffness of the tubular beam in equation (31) with respect to some of the finite lengths Δ_i is given in Table 3. The result shows that the error between equation (31) and FE software (I-DEAS Linear) converges to about 4 per cent when the finite length Δ_i is below 0.1 mm. Thus it seems that the finite length $\Delta_i = 0.1$ mm is reasonable to calculate the torsional stiffness of a tubular beam using equation (31).

Therefore, the results demonstrated that the assumption of representing a torsion beam as a series connection of finite lengths within a constant section would seem to be reasonable.

The contribution of each component to the equivalent spring stiffness (or roll stiffness) in equation (40) and the ADAMS simulation results are shown in Table 4. For the equivalent spring stiffness according to the ADAMS simulation, the average ratio of force to the vertical displacement at the wheel

Table 1 Geometry data of tubular-type torsion beam suspension

Parameter (units)	Values
Distance from the origin to the attachment point P_1 (mm)	2149, 582, −1
Distance from the origin to the shear centre P_2 (mm)	2330.485, 0, 57.166
Distance from the origin to the wheel centre P_3 (mm)	2549, 748, 45
Distance from the origin to the tyre contact point P_4 (mm)	2549, 748, −235
Wheel tread (mm)	1496
Outer diameter of the original tube (mm)	101.6
Thickness of the tubular beam (mm)	2.8
Shear modulus G (kgf/mm^2)	8173.0

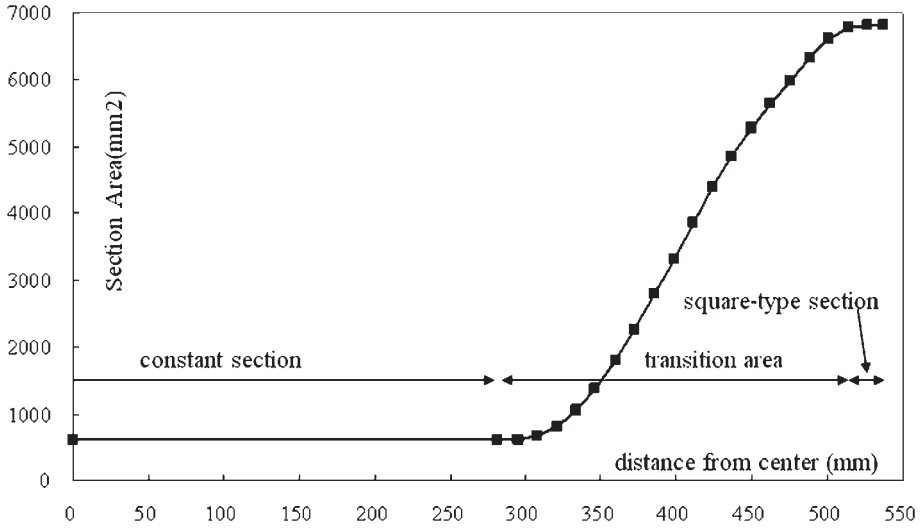

Fig. 8 Cross-section area along the distance from the centre of the tubular beam

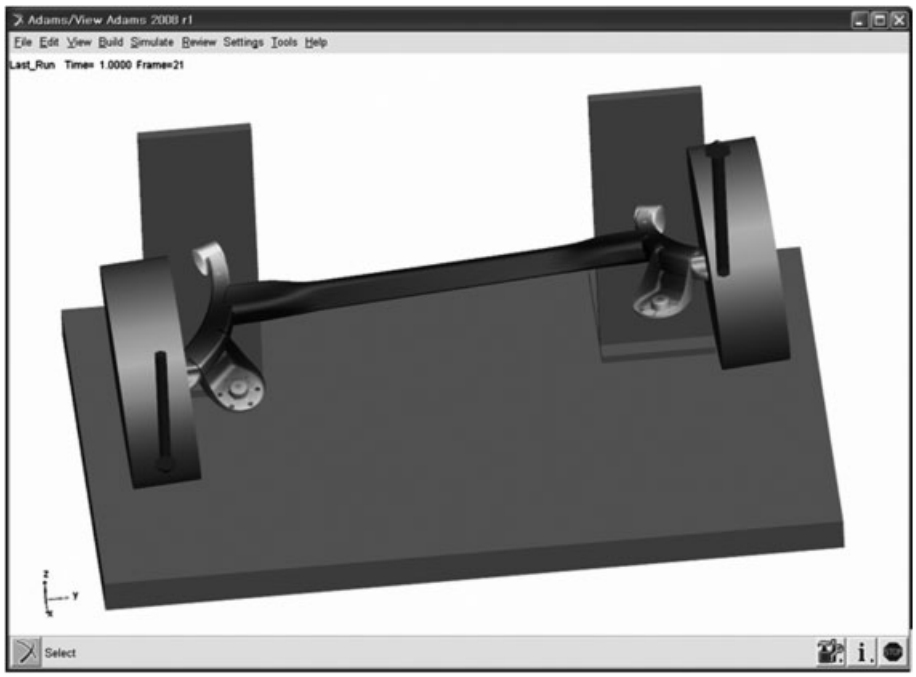

Fig. 9 Torsion beam suspension model in ADAMS/View

centre was calculated while the wheel centre moved 10 mm in a vertical direction in a roll motion. From this table, when compared with the ADAMS results, the proposed analytical equation predicted a reasonable stiffness value, as the error between the two methods (proposed method, 1.739; ADAMS, 1.683) was only 3.3 per cent, which was probably due to an error in calculating the torsional stiffness of the tubular beam in equation (31). When the torsional stiffness of the tubular beam calculated by the I-DEAS Linear analysis in Table 3 was used in equation (40), the error was reduced to around 1.0 per cent.

When considering the contribution of each component to the total equivalent spring stiffness, the torsional stiffness of the tubular beam accounted for 91 per cent of the total spring stiffness, while the bushing stiffness accounted for 9 per cent, making the torsional stiffness the more dominant factor over the conical stiffness. Nontheless, it is still important and reasonable to consider the bushing stiffness to

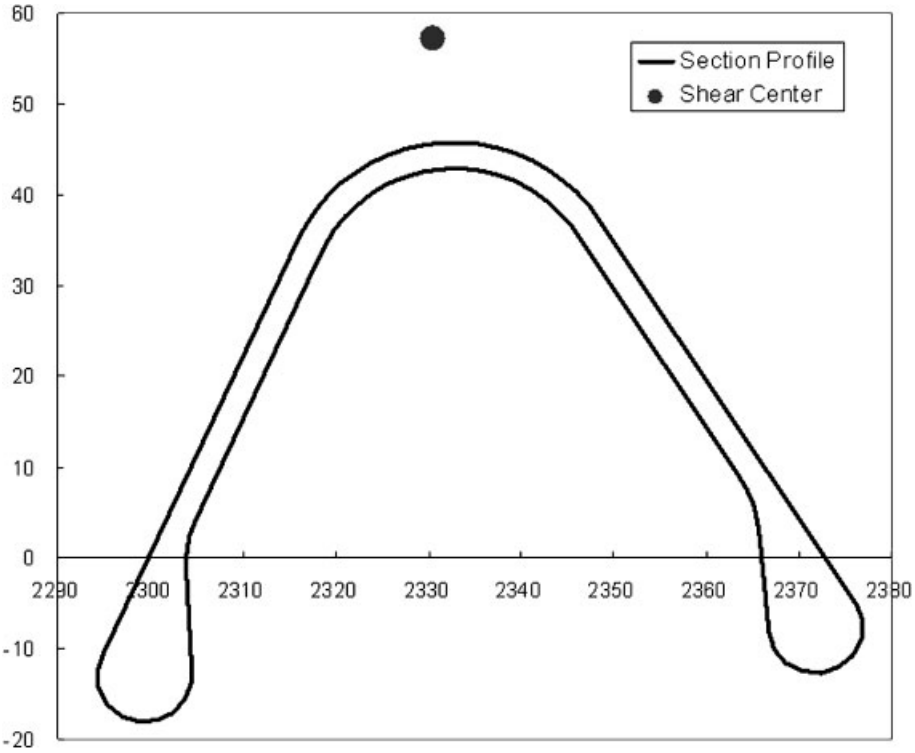

Fig. 10 Shear centre and cross-section profile of the tubular beam

Table 2 Comparison of results with proposed analytical method and ADAMS simulation

	Value obtained by the following methods		
Parameter (units)	Proposed	ADAMS	Error (%)
Roll steer (rad/mm)	$2.226\,726\times10^{-4}$	$2.041\,040\,4\times10^{-4}$	9.1
Roll camber (rad/mm)	$-6.900\,910\times10^{-4}$	$-7.123\,194\,8\times10^{-4}$	3.1
Roll centre height (mm)	187.2	185.8	0.8
Twist angle rate (rad/mm)	$4.428\,668\,3\times10^{-3}$	—	—

Table 3 Comparison of the torsional stiffness K_{tors} in terms of finite length Δ_i

	Proposed value		
Δ_i (mm)	K_{tors} (equation 31) (kgf mm/rad)	Value from I-DEAS Linear (kgf mm/rad)	Error (%)
0.001	$1.610\,95\times10^{5}$	$1.549\,19\times10^{5}$	3.99
0.01	$1.610\,98\times10^{5}$		3.99
0.05	$1.611\,07\times10^{5}$		3.99
0.1	$1.611\,19\times10^{5}$		4.00
0.5	$1.612\,23\times10^{5}$		4.07
1.0	$1.613\,54\times10^{5}$		4.15
2.0	$1.614\,99\times10^{5}$		4.25

Table 4 Comparison of equivalent spring stiffness at the wheel centre

	Value for the following methods			
Component	Proposed equation (40) (contribution (%))		ADAMS	Error (%)
Torsional stiffness of the tubular beam (kgf/mm)	1.580 (90.9%)	1.739 (100%)	1.683	3.3
Torsional stiffness of the bushing (kgf/mm)	0.150 (8.6%)			
Conical stiffness of the bushing (kgf/mm)	0.009 (0.5%)			

predict the equivalent spring stiffness or roll stiffness.

When comparing the required time to obtain the roll properties of the torsion beam model by computer-aided engineering software, the effects of the proposed analytical equations are prominent. It usually takes 2 days to determine the roll properties from meshing of the model and then solving by NASTRAN and ADAMS. However, using the equations proposed in this paper, it will take 30 min at most. Most of the time is required for measuring the section areas at some points of tubular beam and reading the coordinates along the curve of beam section to calculate the shear centre.

In summary, the torsional stiffness and equivalent spring stiffness (or roll stiffness) of a tubular torsion beam system can be effectively predicted from its geometry data and bushing stiffness without the help of multi-body dynamics software.

4 CONCLUSION

This paper proposed an analytical method to calculate the torsional stiffness of a tubular beam with a closed cross-section in a torsion beam rear-suspension system using linear beam theory. Also, a potential energy method is proposed to calculate the equivalent spring stiffness (or roll stiffness) at the wheel centre, based on considering the elastic effect of the torsional stiffness of the tubular beam, together with the torsional and conical stiffnesses of the rubber bushing. The results of the proposed analytical method showed good agreement with the results of an ADAMS simulation in which the flexible body effect was considered.

Furthermore, since the proposed analytical method requires only the geometry of a tubular beam and bushing stiffness, it can provide immediate basic results on the roll properties of a torsion beam, making it an effective tool for design engineers during the initial design stage when there are so many design variables to consider, and which usually takes much time when using multi-body dynamic software, such as ADAMS.

REFERENCES

1 **Bastow, D., Howard, G.,** and **Whitehead, J. P.** *Car suspension and handling,* 4th edition, 2004 (SAE International, Warrendale, USA).

2 **Marsh, A. J., Wolperding, K.,** and **Wille, H. C.** Simulation of the twist beam rear suspension system using flexible bodies in ADAMS. In Proceedings of the 11th European ADAMS User Conference, Frankfurt, Germany, 19–20 November 1996, p. 15 (MSC Software Corporation, Santa Ana, California).

3 **Kim, S., Lee, S., Jung, H.,** and **Lee, C.** Kinematostatic analysis of torsion beam suspension with varying cross section and location of the beam. In Proceedings of the KSAE Conference, May 2002, pp. 813–818 (Korean Society of Automotive Engineers, Seoul).

4 **Fichera, G., Lacagnina, M.,** and **Petrone, F.** Modelling of torsion beam rear suspension by using multibody method. *Multibody System Dynamics*, 2004, **12**, 303–316.

5 **Janarthanam, B., Ghodekar, S. K.,** and **Apte, A. A.** Virtual development of optimum twist beam design configuration for a new generation passenger car. SAE paper 2007-01-3562, 2007.

6 **Kang, J.** Kinematic analysis of torsion beam rear suspension. *Trans. KSAE*, 2004, **12**(5), 146–153.

7 **Sugiura, H., Mizutani, Y.,** and **Nishigaki, H.** First-order analysis for automotive suspension design. *R&D Rev. Toyota CRDL*, 2002, **37**(1), 25–30.

8 **Lyu, N., Park, J., Urabe, H., Tokunaga, H.,** and **Saitou, K.** Design of automotive torsion beam suspension using lumped-compliance linkage model. In Proceedings of the 2006 ASME International Mechanical Engineering Congress and Exposition, Chicago, Illinois, USA, 5–10 November 2006, vol. 119, Part A, paper IMECE2006-15436, pp. 219–228 (ASME, New York).

9 **Satchell, T. L.** The design of trailing twist axles. SAE paper 810420, 1981.

10 **Nikravesh, P. E.** *Computer-aided analysis of mechanical systems*, 1988 (Prentice Hall, Englewood Cliffs, New Jersey).

11 **Gillespie, T. D.** *Fundamentals of vehicle dynamics*, 1992 (Society of Automotive Engineers, New York).

12 **Reimpell, R.** and **Stoll, H.** *The automotive chassis: engineering principles*, 1996 (Society of Automotive Engineers, New York).

13 **Timoshenko, S. P.** and **Goodier, J. N.** *Theory of elasticity*, 3rd edition, 1970 (McGraw-Hill, New York).

14 **Craig, J. I.** Shear center in thin-walled beams lab, 2008, available from http://www.ae.gatech.edu/people/jcraig/classes/ae3145/Lab7/shear-center-theory.pdf.

15 **Ng, T. W.** Shear of thin walled beams. In *MAE 3407 aircraft structures, II: material*, 2009, ch. 7, available from http://biofuturex.com/mae3407/AircraftStruct7.pdf.

16 Bending and torsion of a thin closed section (single cell). In EM 424 Intermediate Mechanics of Materials, 2009, available from http://www.public.iastate.edu/~e_m.424/Closed%20Bending_Torsion.pdf.

17 **Nyhoff, L. R.** and **Leestma, S. C.** *Introduction to FORTRAN 90 for engineers and scientists*, 1996 (Prentice-Hall, Englewood Cliffs, New Jersey).

18 ADAMS/Flex. In *ADAMS 2008 r1 release guide*, 2008, pp. 14–23 (MSC Software Corporation, Santa Ana, California).